2002

Determinants of L-Aspartate and IMP Recognition in Escherichia coli Adenylosuccinate Synthetase

Andrea Gorrell
Iowa State University

Wenyan Wang
Iowa State University

Eric Underbakke
Iowa State University, esu@iastate.edu

Zhenglin Hou
Iowa State University

Richard B. Honzatko
Iowa State University, honzatko@iastate.edu

See next page for additional authors

THE JOURNAL OF BIOLOGICAL CHEMISTRY
Vol. 277, No. 11, Issue of March 15, pp. 8817–8821, 2002
Printed in U.S.A.

Determinants of L-Aspartate and IMP Recognition in *Escherichia coli* Adenylosuccinate Synthetase*

Received for publication, December 11, 2001
Published, JBC Papers in Press, January 7, 2002, DOI 10.1074/jbc.M111810200

Andrea Gorrell‡, Wenyan Wang§, Eric Underbakke¶, Zhenglin Hou‖, Richard B. Honzatko, and Herbert J. Fromm**

From the Department of Biochemistry, Biophysics, and Molecular Biology, Iowa State University, Ames, Iowa 50011

Adenylosuccinate synthetase governs the first committed step in the *de novo* synthesis of AMP. Mutations of conserved residues in the synthetase from *Escherichia coli* reveal significant roles for Val^{273} and Thr^{300} in the recognition of L-aspartate, even though these residues do not or cannot hydrogen bond with the substrate. The mutation of Thr^{300} to alanine increases the K_m for L-aspartate by 30-fold. In contrast, its mutation to valine causes no more than a 4-fold increase in the K_m for L-aspartate, while increasing k_{cat} by 3-fold. Mutations of Val^{273} to alanine, threonine, or asparagine increase the K_m for L-aspartate from 15- to 40-fold, and concomitantly decrease the K_i for dicarboxylate analogues of L-aspartate by up to 40-fold. The above perturbations are comparable with those resulting from the elimination of a hydrogen bond between the enzyme and substrate: alanine mutations of Thr^{128} and Thr^{129} increase the K_m for IMP by up to 30-fold and the alanine mutation of Thr^{301} abolishes catalysis supported by L-aspartate, but has no effect on catalysis supported by hydroxylamine. Structure-based mechanisms, by which the above residues influence substrate recognition, are presented.

In a broad range of organisms and cell types, adenylosuccinate synthetase (IMP:L-aspartate ligase (GDP-forming); EC 6.3.4.4) plays a significant role in *de novo* purine nucleotide biosynthesis, the purine nucleotide cycle, and/or salvage pathways for nucleotides (for reviews, see Refs. 1–3). Adenylosuccinate synthetase converts IMP and L-aspartate to adenylosuccinate using GTP as an energy source. The synthetase from *Escherichia coli* is a homodimer (4). IMP may play an important physiological role in the regulation of synthetase activity by stabilizing the assembly of inactive monomers into active dimers (5, 6). As indicated by investigations, first in kinetics (7–11) and then in x-ray crystallography (12–14), the catalytic mechanism involves a nucleophilic attack on the γ-phosphoryl group of GTP by the 6-oxo group of IMP to form a 6-phosphoryl intermediate of IMP. The displacement of that 6-phosphoryl group by the amino group of L-aspartate generates adenylosuccinate. The synthetase recognizes a limited number of substrate alternatives: 2′-deoxy-IMP and β-D-arabinosyl-IMP substitute for IMP; 2′-deoxy-GTP and GTPγS[1] for GTP; and DL-threo-β-fluoroaspartate, alanine-3-nitronate, cysteine sulfinate, L-alanosine, and hydroxylamine for L-aspartate (7, 15–17).

Four loops, residues 40–53, 120–131, 298–304, and 416–421, undergo conformational transitions in response to active site ligands (12–14, 18–20). Probably as a consequence of these ligand-induced changes, the effect of a mutation in the active site is not easily anticipated from structural information alone. Asn^{38}, for instance, hydrogen bonds with the 5′-phosphoryl group of IMP. However, the mutation of Asn^{38} to alanine has no effect on the K_m for IMP, but reduces k_{cat} by 3 orders of magnitude (21). His^{41} hydrogen bonds with GDP (12), but its mutation to asparagine also increases the K_m for L-aspartate by 7-fold (22). The mutation of Arg^{143}, which hydrogen bonds with the 5′-phosphoryl group of IMP, not only elevates the K_m for IMP by 100-fold, but also the K_m for GTP by 10-fold (23).

Sequence conservation among adenylosuccinate synthetases implicate Thr^{128}, Thr^{129}, Val^{273}, Thr^{300}, and Thr^{301} in important functional roles. All of the above residues, except Val^{273}, belong to flexible loops, which undergo significant conformational change in response to the binding of IMP (loop 120–131) or L-aspartate (loop 298–304). Thr^{128} and Thr^{129} interact with the 5′-phosphoryl group of IMP and Thr^{301} hydrogen bonds directly to the carboxyl group of hadacidin (*N*-formyl *N*-hydroxyglycine; an analogue of L-aspartate). The roles of these residues in substrate recognition can be anticipated on the basis of their interactions in ligated crystal structures. Reasons for sequence conservation at positions 273 and 300, however, are not immediately apparent from crystal structures.

Studies here confirm the anticipated roles of Thr^{128} and Thr^{129} in the recognition of IMP and of Thr^{301} in the recognition of L-aspartate. Thr^{300} supports the recognition of L-aspartate most likely through the influence of its β-branched side chain on the conformation of loop 298–304. Most surprising, however, is the significance of Val^{273} to the recognition of L-aspartate. Its mutation to alanine, threonine, or asparagine causes 15–40-fold increases in the K_m for L-aspartate, while reducing K_i values for analogues of L-aspartate by up to 40-fold. Evidently, Val^{273} is essential in the selection of a catalytically productive conformation of L-aspartate from an ensemble of four-carbon dicarboxylic acids, present at appreciable concentrations *in vivo*.

EXPERIMENTAL PROCEDURES

Materials—Restriction enzymes came from Promega. *Pfu* DNA polymerase and *E. coli* strain XL-1 blue were obtained from Stratagene. *E. coli* strain H1238 (*purA*$^-$) was a gift from Dr. D. Bachman (Genetic

* This work was supported in part by National Institutes of Health Research Grant NS10546 and National Science Foundation Grant MCB-9985565. This is Journal Paper J-19698 of the Iowa Agriculture and Home Economics Experiment Station, Ames, Project 3191, and supported by the Hatch Act and State of Iowa Funds. The costs of publication of this article were defrayed in part by the payment of page charges. This article must therefore be hereby marked "*advertisement*" in accordance with 18 U.S.C. Section 1734 solely to indicate this fact.

‡ Present address: Dept. of Biochemistry and Molecular Biology, Pennsylvania State University, University Park, PA 16802.

§ Present address: Structural Chemistry Dept., Schering-Plough Research Inst., Kenilworth, NJ 07033.

¶ Present address: Biochemistry Dept., University of Wisconsin, Madison, WI 53706.

‖ Present address: Pioneer Hi-Bred International, Inc., Johnston, IA 50131-0552.

** To whom correspondence should be addressed. Tel.: 515-294-4971; Fax: 515-294-0453.

[1] The abbreviation used is: GTPγS, guanosine 5′-3-*O*-(thio)triphosphate.

Center, Yale University, New Haven, CT). Phenyl-Sepharose CL-4B came from Amersham Biosciences, Inc., and hydroxylamine hydrochloride from Fisher Scientific. Other reagents and chemicals came from Sigma, unless specified otherwise.

Expression of Wild-type and Mutant Enzymes—Details regarding the construction of pTrpA are in the literature (21). The *purA* gene in PMS204 was amplified using PCR and *Pfu* DNA polymerase, and subcloned into pTrc99A (Amersham Biosciences, Inc.). The resulting plasmid (pTrpA) was transformed into *E. coli* strain H1238, which cannot express the endogenous synthetase (*purA*$^-$).

Directed Mutations—The *Nco*I-*Pst*I fragment containing *purA* was subcloned into pAlterEXII (Promega). Directed mutagenesis followed the protocol provided by Promega, Inc., using the following primers: 5′-AGCGATCGGCGCCACCGGTCG-3′ for Thr^{128} → Ala, 5′-CGATCGGCACCGCCGGTCGTGGT-3′ for Thr^{129} → Ala, 5′-ACTCCACTCGTGCAGGTGCAGGTC-3′ for Val^{273} → Ala, 5′-ACTCCACTCGTACAGGTGCAGGTC-3′ for Val^{273} → Thr, 5′-ACTCCACTCGTAATGGTGCAGGTC-3′ for Val^{273} → Asn, 5′-GAATTCGGCGCAGCTACGGGGCG-3′ for Thr^{300} → Ala, and 5′-TTCGGCGCAACTGCGGGGCGTCG-3′ for Thr^{301} → Ala.

Nucleotide residues underlined above are mismatched with respect to the wild-type sequence. The sequencing primer used to confirm mutations at positions 128 and 129 was 5′-TCTGAAGCATGTCCGCTGATC-3′, and that used for mutations at positions 273, 300, and 301 was 5′-CTGCTGGATATCGACCACGG-3′. Oligonucleotide synthesis and DNA sequencing (dideoxy dye termination protocol) were done by the Nucleic Acid Facility of Iowa State University. The *Nco*I-*Pst*I fragment with the desired mutation was subcloned into pTrc99A and transformed into *E. coli, purA*$^-$ strain H1238 for expression.

Preparation of Wild-type and Mutant Enzymes—Wild-type and mutant enzymes were purified as described elsewhere (21–24) with the following modifications: The phenyl-Sepharose CL-4B column was washed in succession with solutions of 0.6, 0.4, and 0.2 M ammonium sulfate, buffered by 50 mM potassium phosphate, pH 7.0. Wild-type and mutant synthetases eluted from the column in 0.2 M ammonium sulfate. Appropriate fractions were pooled, concentrated, and dialyzed against 50 mM potassium phosphate, pH 7.0, then further purified by DEAE-TSK high performance liquid chromatography (Toso-Haas). Enzyme purity was monitored by SDS-polyacrylamide electrophoresis (25), and concentrations were determined by the method of Bradford (26), using the reagent from Bio-Rad. Circular dichroism spectra for mutant and wild-type synthetases were taken as described elsewhere (21–23).

Kinetic Assays with L-Aspartate—The ultraviolet difference spectrum of a reaction solution, containing 20 mM Hepes, pH 7.7, 1 mM GTP, 450 μM IMP, 6 mM magnesium chloride, 5 mM L-aspartate, and 20 μg/ml wild-type enzyme was recorded at 25 °C on a GBC UV-visible 918 spectrophotometer, equipped with a Peltier-Effert temperature controller. Kinetic parameters of wild-type and mutant enzymes were determined at 25 °C by monitoring absorbance changes at 290 nm, where the extinction coefficient for the conversion of 1 mol of IMP into adenylosuccinate is 3.51 × 10^6 cm^2/mol. Assay solutions contained 20 mM Hepes, pH 7.7, 5 mM magnesium chloride, and fixed concentrations for two of the three substrates, as appropriate, in the determination of K_m for the remaining substrate (11). Fixed concentrations of GTP, IMP, and L-aspartate were 0.30, 0.50, and 5.0 mM, respectively, unless specified otherwise in tables of kinetic parameters, presented below. 1−200 μg/ml wild-type or mutant enzyme was used in each assay, depending upon its specific activity. Determination of k_{cat} and K_m values employed the program ENZFITTER (27).

Kinetic Assays with Hydroxylamine (NH_2OH)—3 M hydroxylamine was freshly made from hydroxylamine hydrochloride and adjusted to pH 7.7 by the addition of potassium hydroxide. The ultraviolet difference spectrum of a reaction solution containing 20 mM Hepes, pH 7.7, 1 mM GTP, 450 μM IMP, 6 mM magnesium chloride, 400 mM hydroxylamine, and 20 μg/ml wild-type enzyme, was recorded at 25 °C on a GBC UV-visible 918 spectrophotometer, equipped with a Peltier-Effert temperature controller. Kinetic assays were conducted as above at pH 7.7, using fixed concentrations of GTP, IMP, and hydroxylamine of 1, 0.5, and 400 mM, respectively, and 2-mm quartz cuvettes, to offset the strong absorbance of GTP at 280 nm. Determinations of the Hill coefficient for Mg^{2+} came from assays that employed 25 μg/ml wild-type enzyme, 100 mM hydroxylamine, 450 μM IMP, 250 μM GTP, and magnesium chloride from 50 μM to 7 mM. At 280 nm the extinction coefficient for the conversion of 1 mol of IMP into 6-*N*-hydroxy-AMP is 11.7 × 10^6 cm^2/mol. Determination of k_{cat}, K_m, and the Hill coefficient for Mg^{2+} employed the program ENZFITTER (27).

Determination of K_i for Inhibitors—The inhibition constants for succinate, fumarate, and maleate were determined from a 5 × 5 matrix of conditions, which systematically varied L-aspartate and inhibitor concentrations. Assays contained 20 mM Hepes, pH 7.7, 5 mM magnesium chloride, 500 μM IMP, and 300 μM GTP. Enzyme concentrations were 4, 30, 20, and 66 μg/ml for the wild-type, Val^{273} → Ala, Val^{273} → Asn, and Val^{273} → Thr enzymes, respectively. L-Aspartate varied from one half to 5 times its K_m (depending upon the mutant examined), and inhibitor concentrations varied from 0 to 15 mM succinate, from 0 to 16.7 mM fumarate, or from 0 to 10 mM maleic acid. Kinetic parameters for inhibition were determined by linear regression, using the MINITAB program and a value for α of 2.0 (28).

Sequence Comparisons—The Biology WorkBench of the San Diego Supercomputing Center (workbench.sdsc.edu) served as a platform in sequence similarity searches (29) and multiple sequence alignments (30). Sequences of adenylosuccinate synthetases were identified initially by their match to the 9-residue P-loop of the synthetase (single-letter amino acid sequence: QWGDEGKGK).

RESULTS

Conservation of Target Residues—Positions 129 and 273 are threonine and valine, respectively, in all sequences of adenylosuccinate synthetases extracted from the Protein Information Resource data base (a total of 45 entries), whereas positions 128 and 301 are threonine in 44 sequences (serine was the alternative residue). In 32 of 45 sequences, position 300 is threonine, the alternative residue types being valine (10 instances), serine (2 instances), and asparagine (1 instance). Sequences within the adenylosuccinate synthetase family exhibit at least 40% identity for any pairwise alignment.

Purity and Secondary Structure of Mutant Enzymes—The mutant and wild-type enzymes migrate comparably on phenyl-Sepharose and DEAE columns. All proteins were at least 95% pure on the basis of SDS-polyacrylamide gel electrophoresis. Circular dichroism spectra of all enzymes were identical from

TABLE I

Kinetic parameters for wild-type and mutant adenylosuccinate synthetases

See text for conditions of assay. K_m^{GTP}, K_m^{IMP}, and K_m^{Asp} are the Michaelis constants for GTP, IMP, and L-aspartate, respectively.

Enzyme[a]	k_{cat}	K_m^{GTP}	K_m^{IMP}	K_m^{Asp}	k_{cat}/K_m^{GTP}	k_{cat}/K_m^{IMP}	k_{cat}/K_m^{Asp}
	s^{-1}	μM	μM	mM	s^{-1} mM^{-1}	s^{-1} mM^{-1}	s^{-1} mM^{-1}
Wild-type	1.00 ± 0.05	26 ± 2	28 ± 1	0.23 ± 0.04	38 ± 4	36 ± 3	4.4 ± 0.8
Thr^{128} → Ala[b]	0.46 ± 0.03	54 ± 6	310 ± 50	0.17 ± 0.02	9 ± 1	1.5 ± 0.3	2.7 ± 0.4
Thr^{129} → Ala[c]	0.42 ± 0.01	1700 ± 60	890 ± 70	0.24 ± 0.01	0.25 ± 0.01	0.47 ± 0.04	1.75 ± 0.08
Thr^{300} → Ala[d]	0.64 ± 0.04	170 ± 10	19 ± 1	6.2 ± 0.7	3.9 ± 0.4	34 ± 3	0.10 ± 0.01
Thr^{300} → Val	3.3 ± 0.2	56 ± 6	33 ± 3	0.82 ± 0.02	60 ± 7	100 ± 10	4.1 ± 0.2
Val^{273} → Ala[d,e]	1.00 ± 0.1	31 ± 3	17 ± 2	7 ± 1	32 ± 5	59 ± 9	0.14 ± 0.03
Val^{273} → Asn[d,e]	0.050 ± 0.001	21 ± 2	24 ± 2	9 ± 2	2.4 ± 0.2	2.1 ± 0.2	0.006 ± 0.001
Val^{273} → Thr[d,e]	1.99 ± 0.02	45 ± 7	43 ± 4	3.4 ± 0.2	44 ± 1	46 ± 6	0.61 ± 0.07

[a] Observed no catalytic activity for the Thr^{301} → Ala enzyme under conditions specified in the text.
[b] Employed fixed concentrations of 0.25 mM IMP and 0.45 mM GTP.
[c] Employed fixed concentrations of 6 mM IMP and 0.60 mM GTP.
[d] Employed fixed concentration of 25 mM L-aspartate.
[e] Assayed with 25 mM magnesium chloride while varying the concentration of L-aspartate.

TABLE II
Inhibition constants for wild-type and position 273 mutant enzymes

See text for details regarding conditions of assay. K_i for various inhibitors is defined by Equation 1 in the text.

Enzyme	K_i		
	Succinate	Fumarate	Maleate
	μM	μM	μM
Wild-type	890 ± 50	NI[a]	3100 ± 80
$Val^{273} \rightarrow Ala$	NI[a]	180 ± 40	1000 ± 200
$Val^{273} \rightarrow Asn$	NI[a]	40 ± 10	210 ± 8
$Val^{273} \rightarrow Thr$	80 ± 10	640 ± 80	78 ± 5

[a] Noninhibitory to a concentration of 10 mM.

TABLE III
Kinetic parameters of wild-type and mutant synthetases with hydroxylamine

See text for details regarding the conditions of assay.

Enzyme	k_{cat}	$K_m^{hydroxylamine}$	K_m^{GTP}	K_m^{IMP}
	s^{-1}	mM	μM	μM
Wild-type	0.50 ± 0.09	230 ± 80	190 ± 20	66 ± 7
$Thr^{301} \rightarrow Ala$	0.24 ± 0.04	91 ± 3	57 ± 7	320 ± 90
$Val^{273} \rightarrow Ala$	0.21 ± 0.02	255 ± 60	140 ± 40	140 ± 20
$Val^{273} \rightarrow Asn$	0.29 ± 0.08	110 ± 70	180 ± 30	113 ± 7
$Val^{273} \rightarrow Thr$	0.080 ± 0.002	140 ± 30	74 ± 8	77 ± 6

200 to 260 nm (data not shown), indicating no major changes in secondary structure.

Kinetics with L-Aspartate—K_m^{Asp} and k_{cat} values for the wild-type, $Thr^{128} \rightarrow Ala$, and $Thr^{129} \rightarrow Ala$ enzymes are comparable (Table I). In contrast, the mutation of Thr^{128} to alanine increases K_m^{IMP} and K_m^{GTP} by 10- and 2-fold, respectively, and the mutation of Thr^{129} to alanine increases K_m^{IMP} and K_m^{GTP} by 30- and 80-fold, respectively. Mutations of position 273 have little effect on K_m^{GTP} and K_m^{IMP}, but increase K_m^{Asp} by 30-, 40-, and 15-fold for the alanine, asparagine, and threonine mutations, respectively. Values of k_{cat} for the $Val^{273} \rightarrow Ala$ and $Val^{273} \rightarrow Thr$ enzymes are similar (2-fold less and 3-fold greater than, respectively) to that of the wild-type enzyme, but the mutation of Val^{273} to asparagine causes a 20-fold reduction in k_{cat}. The mutation of Thr^{300} to alanine elevates K_m^{GTP} by 5-fold and K_m^{Asp} by 30-fold. In contrast, K_m^{GTP} and K_m^{IMP} increase by 2-fold or less as a result of the mutation of Thr^{300} to valine, and k_{cat} and K_m^{Asp} increase by only 3-fold. The mutation of Thr^{301} to alanine results in the complete loss of activity under conditions employed here (20 mM Hepes, pH 7.7, 1 mM GTP, 500 μM IMP, 6 mM Mg^{2+}, 25 mM L-aspartate, 200 μg/ml protein).

Kinetic parameters for the inhibition of wild-type enzyme and position 273 mutant synthetases by succinate, fumarate, and maleate vary over a broad range of affinities (Table II). All kinetic mechanisms of inhibition are competitive with respect to L-aspartate, fitting to Equation 1 with a goodness-of-fit below 5%.

$$1/V = (1/V_{max}) \cdot (1 + K_a/A + K_{ia} \cdot I/K_i \cdot A) \qquad \text{(Eq. 1)}$$

In Equation 1, v is the initial velocity, V_{max} is the maximal velocity, A is the concentration of L-aspartate, I is the inhibitor concentration, K_a is the Michaelis constant for L-aspartate, K_i is the dissociation constant for the inhibitor, and K_{ia} is the dissociation constant for L-aspartate. All of the position 273 mutants exhibit significant decreases in K_i relative to the wild-type enzyme for at least one of the alternative dicarboxylic acids (Table II). Each of the dicarboxylic acids, however, were more effective inhibitors (by up to 40-fold) of the $Val^{273} \rightarrow Thr$ enzyme relative to the wild-type synthetase.

Kinetics with Hydroxylamine—Ala^{301}, Ala^{273}, Thr^{273}, Asn^{273}, and wild-type enzymes exhibit similar kinetic parameters when assayed with hydroxylamine (Table III). $K_m^{hydroxylamine}$, K_m^{GTP}, and K_m^{IMP} vary over a 3-fold range, whereas k_{cat} varies 6-fold among the enzymes of Table III. The Hill coefficient for Mg^{2+}, however, falls from 2 to unity when hydroxylamine replaces L-aspartate (data not shown).

DISCUSSION

The residues studied here cluster in the vicinity of the L-aspartate and IMP binding sites (Fig. 1). The side chain of Thr^{128} hydrogen bonds with Asp^{114}, facilitating hydrogen bonds between the side chain and backbone amide of Thr^{129} with the 5′-phosphoryl group of IMP. The side chain of Thr^{300} approaches and may hydrogen bond weakly with backbone carbonyl 38 and the side chain of His^{53}. The backbone amide

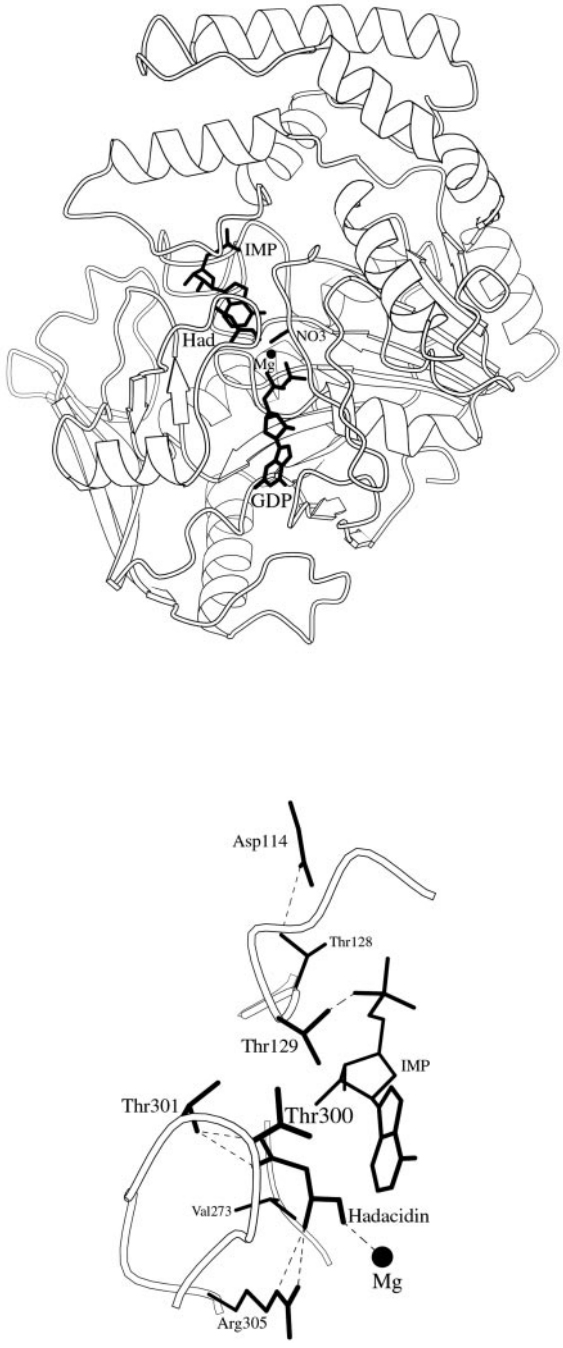

FIG. 1. **Relative positions of residues subject to mutation.** *Top*, location of residues relative to a single subunit of the adenylosuccinate synthetase dimer; *bottom*, a more detailed view showing specific interactions. Donor-acceptor interactions and selected nonbonded contacts are indicated by *dashed lines*. Coordinates are from the GDP·IMP·NO_3^-·Mg^{2+}·hadacidin complex (Ref. 37; Protein Data Base accession code 1cib). This drawing was done with MOLSCRIPT (38).

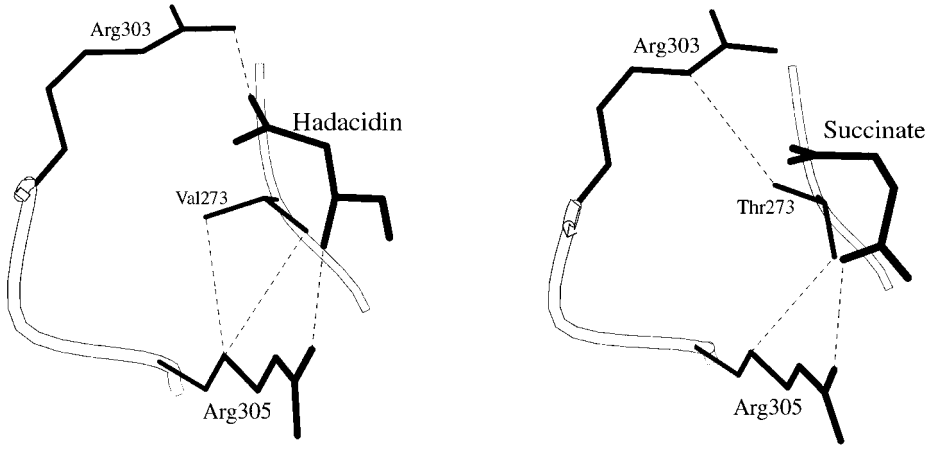

FIG. 2. **Interactions of amino acid residue 273.** Val^{273} makes allowable nonbonded contacts with Arg^{305} at the cost of an unfavorable χ^1 torsion angle in the GDP·IMP·NO_3^-·Mg^{2+}·hadacidin complex (Protein Data Base accession code 1cib; *left*). Thr^{273} makes allowable nonbonded contacts with Arg^{303} and Arg^{305}, while adopting a favorable χ^1 torsion angle in the GDP·IMP·Mg^{2+}·succinate complex, but Arg^{303} may not hydrogen bond with the carboxyl group of succinate (*right*). Donor-acceptor interactions and selected nonbonded contacts are indicated by *dashed lines*. This drawing was done with MOLSCRIPT (38).

and side chain of Thr^{301} hydrogen bond with the carboxyl group of hadacidin (an analogue of L-aspartate). The conformation of bound hadacidin in crystallographic complexes is consistent with an intramolecular hydrogen bond between the β-carboxyl and α-amino groups of L-aspartate (3, 12). The β-carboxyl group may then abstract a proton from the α-amino group of L-aspartate in catalyzing the second step of the synthetase reaction. The side chain of Val^{273} makes nonbonded contacts with hadacidin and with the aliphatic methylene carbons of the side chain of Arg^{305}. Although side chains larger than an isopropyl group at position 273 could come into steric conflict with L-aspartate, there are no steric conflicts in the substitution of side chains of smaller or similar size. The backbone carbonyl of Val^{273} hydrogen bonds with the 2′-hydroxyl group of IMP, but this interaction may not be important as 2′-deoxy-IMP is a good substrate for the synthetase (31). The side-chain conformation of Val^{273} is unfavorable ($\chi^1 \sim 240°$, an eclipsed conformation; Fig. 2). Efforts to build and refine (by simulated annealing), the side chain in a staggered conformation ($\chi^1 \sim 60°$, 180°, or 300°) return the unfavorable torsion angle.[2] Staggered conformations for Val^{273} cause unacceptable contacts with backbone carbonyl 273 and/or the CG atom of Arg^{305}.

$Thr^{128} \rightarrow$ Ala and $Thr^{129} \rightarrow$ Ala synthetases exhibit 10- and 30-fold increases in K_m^{IMP}, respectively, while retaining wild-type levels of activity. Presumably, the hydrogen bond between Thr^{128} and Asp^{114} stabilizes the ligand-bound conformation of loop 120−131, and facilitates interactions between Thr^{129} and the 5′-phosphoryl group of IMP. Evidently, interactions involving Thr^{128} and Thr^{129} do little to stabilize the transition state (k_{cat} falls only 2-fold because of these mutations). In this regard, the effects of mutations at positions 128 and 129 and at Arg^{143} are similar. The side chain of Arg^{143} from a symmetry-related monomer of the synthetase dimer hydrogen bonds with the 5′-phosphoryl group of IMP. The mutation of Arg^{143} to leucine or lysine results in a 100-fold increase in K_m^{IMP} and no change in k_{cat} (6). In contrast, the mutation of Asn^{38}, which also hydrogen bonds with the 5′-phosphoryl group of IMP, has no effect on K_m^{IMP}, but causes a 1000-fold decrease in k_{cat} (21).

The 60-fold increase in K_m^{GTP} relative to the wild-type enzyme for the $Thr^{129} \rightarrow$ Ala mutant must come from an indirect mechanism, as Thr^{129} and GTP are separated by more than 10 Å. A 10-fold increase in K_m^{GTP} was observed for the $Arg^{143} \rightarrow$ Leu synthetase (6). Correlated changes in K_m^{IMP} and K_m^{GTP} probably stem from binding synergism between IMP and GTP, which may originate from the interaction of Asn^{38} with the 5′-phosphoryl group of IMP. In a crystal structure of an IMP-synthetase complex (32), loop 40−53 adopts the conformation of the GDP-bound synthetase in the absence of guanine nucleotide. IMP alone, through its interaction with Asn^{38}, can stabilize the GDP-bound conformation of loop 40−53. Correlated changes in K_m^{IMP} and K_m^{GTP} because of mutations at positions 129 and 143, then, may stem from a perturbation of the Asn^{38}-IMP interaction and a concomitant loss in the ability of IMP to drive conformational changes in loop 40–53.

The significant effects on K_m^{Asp} and/or k_{cat} resulting from mutations of threonines 300 and 301 to alanine are in harmony with those observed in mutations of Arg^{303}, and Arg^{304} and Arg^{305} to leucine (33). Crystallographic structures implicate loop 298−304 in the recognition of the β-carboxyl group of L-aspartate (3, 12). The 30-fold increase in K_m^{Asp} for the $Thr^{300} \rightarrow$ Ala synthetase may arise in part from the loss of weak hydrogen bonds involving the side chain of Thr^{300}, but other factors are involved here as well. The β-branched side chain at position 300 limits allowable main-chain torsion angles relative to the methyl group of alanine. The $Thr^{300} \rightarrow$ Val enzyme retains the conformational restraints because of the β-branched side chain, but eliminates side-chain hydrogen bonds. The consequence is only a 3-fold increase in K_m^{Asp} and an increase in k_{cat} of 300%. The modest effects of the $Thr^{300} \rightarrow$ Val mutation are consistent with the presence of valine at position 300 in 25% of known sequences for the synthetase. The 5-fold increase in K_m^{GTP} resulting from the mutation of Thr^{300} to alanine may reflect binding synergism between L-aspartate and GTP. GTP/L-aspartate binding synergism may stem in part from the coordination of each ligand to a common Mg^{2+}. In addition, a series of crystal structures (14) demonstrate enhanced interactions between Arg^{305} (which putatively binds to the α-carboxyl group of L-aspartate) and the α-phosphoryl group of the guanine nucleotide in the presence of hadacidin (the L-aspartate analogue).

As the $Thr^{301} \rightarrow$ Ala synthetase is inactive in assays using L-aspartate, we are unable to determine whether the loss of activity is the result of an effect on k_{cat} or to a large increase in K_m^{Asp}. If the mutation of Thr^{301} to alanine eliminates critical hydrogen bonds with the β-carboxyl group of L-aspartate, as inferred by crystal structures and model building (3, 12), then the $Thr^{301} \rightarrow$ Ala mutant enzyme and the wild-type enzyme should respond comparably to hydroxylamine as an alternative substrate. Indeed, kinetic parameters for the $Thr^{301} \rightarrow$ Ala mutant are similar to those of the wild-type enzyme when hydroxylamine is used in place of L-aspartate (Table III). The apparent saturation effect, observed with increasing concentrations of hydroxylamine, may be a consequence then of reduced specific activity of the synthetase at high ionic strength. So, in fact, the reaction involving hydroxylamine may be diffusion-controlled.

The reduced Hill coefficients in reactions that employ hydroxylamine reaffirm the correlated binding of L-aspartate and

[2] Z. Hou and R. B. Honzatko, unpublished results.

a second Mg^{2+} in the kinetic mechanism of the synthetase (34). Evidently, only one Mg^{2+} participates in the hydroxylamine reaction, whereas two are involved in the L-aspartate reaction. Kang and Fromm (34) suggest that a second Mg^{2+} binds to the carboxyl groups of L-aspartate, to reduce the pK_a of its α-amino group. An alternative model puts the second Mg^{2+} between the α-carboxyl group of L-aspartate and the side chain of Asp^{13}, to offset the effects of an unacceptable nonbonded contact between these groups (3). Both models are consistent with the reduced Hill coefficient observed in the presence of hydroxylamine. Mg^{2+} may not coordinate hydroxylamine effectively, but its pK_a (8.0) is low enough to support catalysis at pH 7.7 (pH of optimal activity) without the influence of a second Mg^{2+}.

Although only nonbonded contacts are evident in crystal structures between Val^{273} and hadacidin, the mutation of Val^{273} to alanine causes a 30-fold increase in K_m^{Asp}. As the mutation puts a small side chain in place of a larger one, unfavorable steric interactions with the substrate are unlikely. Furthermore, the productive binding of L-aspartate to the Ala^{273} mutant and wild-type enzymes must be nearly identical, as K_m^{GTP} (which reflects L-aspartate/GTP-binding synergism) and k_{cat} are unchanged. Mutation to a larger side chain ($Val^{273} \rightarrow$ Asn) causes a 40-fold increase in K_m^{Asp} and a 20-fold reduction in k_{cat}, suggesting a perturbation in the productive binding of L-aspartate, resulting perhaps from the steric effects from a side chain with increased size. The isosteric mutation $Val^{273} \rightarrow$ Thr, however, still causes a 15-fold increase in K_m^{Asp}, whereas k_{cat} actually increases 200%.

Inhibition of position 273 mutants by dicarboxylic acids provides a measure of insight as to how Val^{273} functions in substrate recognition. Fumarate is a potent inhibitor of the Ala^{273} and Asn^{273} mutant enzymes, but has no effect on the wild-type enzyme, and similarly succinate and maleate become potent inhibitors of the Thr^{273} mutant enzyme. The active sites of position 273 enzymes generally recognize a more diverse set of dicarboxylic acids than does the wild-type active site. This broadened recognition for dicarboxylic acids may allow L-aspartate to bind in different modes to the active sites of the position 273 mutants. Productive binding for L-aspartate is retained in the Thr^{273} and Ala^{273} mutant enzymes, but other, nonproductive binding modes may be important. These nonproductive binding modes may include, for instance, the ligation of the β-carboxyl group of L-aspartate to the active site Mg^{2+} (backward binding) and/or the binding of L-aspartate in a conformation that does not permit the formation of an intramolecular hydrogen bond between its β-carboxyl and α-amino groups. Hence, the K_m^{Asp} may increase for position 273 mutants enzymes because of competition between productive and nonproductive binding modes of the substrate.

The kinetic properties of the above mutations are clearly consistent with the absolute sequence conservation of valine at position 273. In fact, the selective pressures that retain position 273 as valine are now evident. In *vivo* concentrations of fumarate, succinate, and L-aspartate in *E. coli* are ~0.4, 0.4, and 2 mM (35, 36). The mutations at position 273, presented here, are relatively conservative, yet each generates an enzyme that has a K_m^{Asp} at least 5-fold higher than intracellular concentrations of L-aspartate and vastly improved binding affinities for succinate and fumarate. Under physiological conditions, then, the position 273 mutant enzymes are inactive.

In preliminary crystal structures of the Thr^{273} synthetase in complexes with succinate·IMP·GDP·Mg^{2+} and maleate·IMP·GDP·Mg^{2+} at 2-Å resolution,[3] the active site is not substantially altered by the mutation. Succinate and maleate coordinate to Mg^{2+} and hydrogen bond to loop 298–304, as observed in the hadacidin-ligated active site of the wild-type enzyme. Thr^{273} has a χ^1 angle of 300°, a rotation of 60° relative to the χ^1 angle for the side chain of Val^{273} of the wild-type enzyme (Fig. 2). The side chain of Thr^{273} now makes nonbonded contacts with both Arg^{303} and Arg^{305}, but no hydrogen bonds. Arg^{303} approaches, but may not hydrogen bond with, succinate. These subtle differences in conformation may be caused by the mutation at position 273 or to the replacement of hadacidin with succinate/maleate. Information from the hadacidin complex of the Thr^{273} enzyme is necessary before definitive conclusions are possible. Nonetheless, the functional consequences of the mutation of Val^{273} to threonine are not the result of gross conformational changes at the active site and/or hydrogen bonding of the threonine hydroxyl group OG1.

[3] C. Iancu, E. Underbakke, and R. B. Honzatko, unpublished results.

REFERENCES

1. Stayton, M. M., Rudolph, F. B., and Fromm, H. J. (1983) *Curr. Top. Cell Regul.* **22,** 103–141
2. Honzatko, R. B., Stayton, M. M., and Fromm, H. J. (1999) *Adv. Enzymol. Relat. Areas Mol. Biol.* **73,** 57–102
3. Honzatko, R. B., and Fromm, H. J. (1999) *Arch. Biochem. Biophys.* **370,** 1–8
4. Poland, B. W., Silva, M. M., Serra, M. A., Cho, Y., Kim, K. H., Harris, E. M. S., and Honzatko, R. B. (1993) *J. Biol. Chem.* **268,** 25334–25342
5. Kang, C., Kim, S., and Fromm, H. J. (1996) *J. Biol. Chem.* **271,** 29722–29728
6. Wang, W., Gorrell, A., Honzatko, R. B., and Fromm, H. J. (1997) *J. Biol. Chem.* **272,** 7078–7084
7. Lieberman, I. (1956) *J. Biol. Chem.* **223,** 327–339
8. Fromm, H. J. (1958) *Biochim. Biophys. Acta* **29,** 255–262
9. Bass, M. B., Fromm, H. J., and Rudolph, F. B. (1984) *J. Biol. Chem.* **259,** 12330–12333
10. Cooper, B. F., Fromm, H. J., and Ruldoph, F. B. (1986) *Biochemistry* **25,** 7323–7327
11. Rudolph, F. B., and Fromm, H. J. (1969) *J. Biol. Chem.* **244,** 3832–3839
12. Poland, B. W., Fromm, H. J., and Honzatko, R. B. (1996) *J. Mol. Biol.* **264,** 1013–1027
13. Poland, B. W., Bruns, C., Fromm, H. J., and Honzatko, R. B. (1997) *J. Biol. Chem.* **272,** 15200–15205
14. Choe, J. Y., Poland, B. W., Fromm, H. J., and Honzatko, R. B. (1999) *Biochemistry* **38,** 6953–6961
15. Porter, D. J. T., Rudie, N. G., and Bright, H. J. (1983) *Arch. Biochem. Biophys.* **225,** 157–163
16. Gale, G. R., and Smith, A. B. (1968) *Biochem. Pharm.* **17,** 2495–2498
17. Casey, P. J., Abeles, R. H., and Lowenstein, J. M. (1986) *J. Biol. Chem.* **261,** 13637–13642
18. Fonné-Pfister, R., Chemla, P., Ward, E., Girardet, M., Kreuz, K. E., Honzatko, R. B., Fromm, H. J., Schaer, H. P., Gruetter, M. G., and Cowan-Jacob, S. W. (1996) *Proc. Natl. Acad. Sci. U. S. A.* **93,** 9431–9436
19. Poland, B. W., Hou, Z., Bruns, C., Fromm, H. J., and Honzatko, R. B. (1996) *J. Biol. Chem.* **271,** 15407–15413
20. Poland, B. W., Lee, S.-F., Subramanian, M. V., Siehl, D. L., Anderson, R. J., Fromm, H. J., and Honzatko, R. B. (1996) *Biochemistry* **35,** 12753–15759
21. Wang, W., Gorrell, A., Hou, Z., Honzatko, R. B., and Fromm, H. J. (1998) *J. Biol. Chem.* **273,** 16000–16004
22. Kang, C., Sun, N., Poland, B. W., Gorrell, A., Honzatko, R. B., and Fromm, H. J. (1997) *J. Biol. Chem.* **272,** 11881–11885
23. Wang, W., Hou, Z., Honzatko, R. B., and Fromm, H. J. (1997) *J. Biol. Chem.* **272,** 16911–16916
24. Bass, M. B., Fromm, H. J., and Stayton, M. M. (1987) *Arch. Biochem. Biophys.* **256,** 335–342
25. Laemmli, U. K. (1970) *Nature* **227,** 680–685
26. Bradford, M. M. (1976) *Anal. Biochem.* **72,** 248–254
27. Leatherbarrow, R. J. (1977) *Enzfitter: A Non-linear Regression Data Analysis Program for the IBM PC*, pp. 13–75, Elsevier Science Publishers B.V., Cambridge, United Kingdom
28. Lui, F., and Fromm, H. J. (1990) *J. Biol. Chem.* **265,** 7401–7406
29. Altschul, S. F., Madden, T. L., Schaffer, A. A., Zhang, J., Zhang, Z., Miller, W., and Lipman, D. J. (1997) *Nucleic Acids Res.* **25,** 3389–3402
30. Thompson, J. D., Higgins, D. G., Gibson, T. J. (1994) *Nucleic Acids Res.* **22,** 4673–4680
31. Spector, T., and Miller, R. L. (1976) *Biochim. Biophys. Acta* **445,** 509–517
32. Hou, Z., Wang, W., Fromm, H. J., and Honzatko, R. B. (2002) *J. Biol. Chem.* **277,** in press
33. Wang, W., Poland, B. W., Honzatko, R. B., and Fromm, H. J. (1995) *J. Biol. Chem.* **270,** 13160–13163
34. Kang, C., and Fromm, H. J. (1995) *J. Biol. Chem.* **270,** 15539–15544
35. Lowry, O. H., Carter, J., Ward, J. B., and Glaser, L. (1971) *J. Biol. Chem.* **246,** 6511–6521
36. Siegel, W. H., Donohue, T., and Bernlohr, R. W. (1977) *Appl. Env. Microbiol.* **34,** 512–517
37. Hou, Z., Cashel, M. C., Fromm, H. J., and Honzatko, R. B. (1999) *J. Biol. Chem.* **274,** 17505–17510
38. Kraulis, J. (1991) *J. Appl. Crystallogr.* **24,** 946–950

Determinants of l-Aspartate and IMP Recognition in*Escherichia coli* Adenylosuccinate Synthetase

Andrea Gorrell, Wenyan Wang, Eric Underbakke, Zhenglin Hou, Richard B. Honzatko and Herbert J. Fromm

J. Biol. Chem. 2002, 277:8817-8821.
doi: 10.1074/jbc.M111810200 originally published online January 7, 2002
